Functional organization underlying superior performance in a memory champion

Roselyne J. Chauvin[1,2,✉] · Annie Zheng[1] · Athanasia Metoki[1,2] · Samuel R. Krimmel[1,2] · Ashley Nielsen[1] · Anxu Wang[1,2,3] · Philip N. Cho[1,2] · Noah J. Baden[1,2] · Daniel Bower[1,2] · Kristen M. Scheidter[1,2] · Julia S. Monk[1,2] · Forrest I. Whiting[1,2] · Babatunde Adeyemo[1,2]· Scott Marek[2,4,5]· Benjamin P. Kay[1,2] · Henry L. Roediger[6]· Kathleen McDermott[5,6]· Steven M. Nelson[7,8]· Adrian W. Gilmore[9] · Deanna M. Barch[4,5,6]· Timothy O. Laumann[2,4] · Evan M. Gordon[2,5] · Nico U.F. Dosenbach[1,2,3,5,6,10]

[1] Department of Neurology, Washington University School of Medicine, St. Louis, MO 63110
[2] Allied Labs for Imaging Guided Neurotherapies (ALIGN), Washington University School of Medicine, St. Louis, MO, USA
[3] Department of Biomedical Engineering, Washington University in St. Louis, MO 63130
[4] Department of Psychiatry, Washington University School of Medicine, St. Louis, MO 63110
[5] Mallinckrodt Institute of Radiology, Washington University School of Medicine, St. Louis, MO 63110
[6] Department of Psychological and Brain Sciences, Washington University in St. Louis, St. Louis, MO, USA
[7] Masonic Institute for the Developing Brain, University of Minnesota Medical School, Minneapolis, MN, USA
[8] Department of Pediatrics, University of Minnesota, Minneapolis, MN, USA
[9] Department of Psychological and Brain Sciences, University of Delaware, Newark, DE, 19716, United States of America.
[10] Department of Pediatrics, Washington University School of Medicine, St. Louis, MO 63110

✉ Correspondence: Roselyne J Chauvin <chauvin@wustl.edu>

Summary

Memory athletes can achieve superior performance (e.g., memorizing 339 digits in 5 minutes) with extensive daily training, by converting abstract information into vivid scenes, and placing them along a mental path, that is then retraced at recall (Method of Loci). Understanding the brain mechanisms underlying such training-dependent performance could suggest novel brain-based approaches to improve learning and cognitive performance in other domains. As each memory athlete uses individual-specific, personalized training techniques, it has been challenging to study them at the group level. Fortunately, precision functional mapping (PFM) which uses repeated sampling of resting state functional connectivity and task fMRI, enables detailed study of individual brains. Here, we map the brain organization of a 6-time U.S. Memory Champion (>13 hours fMRI) and compare it to control data. We observe focal functional connectivity differences in the memory champion's retrosplenial, extrastriate visual, and dorsal frontal cortex (area 55b), as well as in the caudate. These suggest additional recruitment of scene and semantic processing in the athlete, alongside a stronger integration of the caudate with memory-related networks. A control rote memorization task elicits typical activation patterns in the athlete, but when using the Method of Loci, his pattern on activation differs: his hippocampal activation was larger during recall than encoding and he recruited regions showing connectivity differences compared to controls. His unique circuit for Method of Loci, incorporates regions typically used for navigation, scene processing, language and associative learning.

Main

Working memory, the ability to maintain and manipulate items in the short-term represents a bottleneck for learning[1]. Newly learned information is primarily thought to transition to long-term storage via the hippocampus[2,3]. Several large-scale functional neural networks are important for different aspects of long-term memory and recollection, including the default-mode network (DMN), which is important for self-referential processing[4], and the parietal memory network (PMN) known to be involved in recall[5,6]. Spatial memory, important for navigation[7], is supported by the context-association network (CAN) which includes retrosplenial[8,9], parahippocampal[10] and entorhinal cortex[11]. Memory consolidation can be enhanced by reward circuitry, including the salience network, which signals the importance of new information[12] and which activity has recently been closely associated with the PMN[13,14]. Within the reward circuit, the caudate is particularly involved in linking stimuli and responses during conditioning and rule-based learning[12,15].

Our ability to memorize is limited by a small working memory span[16]. Memory athletes demonstrate that this limitation can be overcome. The 6-time US Memory Champion, for example, was able to memorize the order of a deck of 52 cards in 40.65 seconds, establishing a US record at age 27, in a challenge called 'speed card' (Figure 1a). This Memory Champion is a remarkable example of exceptional adult skill acquisition. While he did not have a great memory when young[17], as an adult, he became the U.S. Memory Champion within two years of starting training in memory techniques, eventually becoming the holder of the most U.S. Memory Champion titles (6x). With continued training, his memorization skills have improved over time. For example, he could memorize 178 digits in 5 minutes at age 27, and 339 digits by age 30 (Figure 1b).

In contrast to individuals with savant syndromes that show remarkable innate memory capabilities[18], memory athletes use mnemonic techniques and hours of daily training. A core mnemonic technique used by memory athletes is the Method of Loci[19]. In this technique, items to be memorized are placed along a mental path that can be mentally navigated in order to recall information (e.g. within the person's house, one could begin in the kitchen, travel to the living room, and then up the stairs to the bedroom, with each location as a memory locus). To increase the number of items memorized (more than one per mental path locus), Memory Athletes use semantic or visual associations and stories to link items. Part of the training is to create an encoding system that is most memorable for them (e.g., types of images, character references). For example, information can be chunked using a predefined compression system in which each abstract item (such as a card or a digit) is pre-associated with something more easily visualizable (e.g. typically a person, an action, and an object) that are then combined into a visual scene (e.g. person of item 1: ace of spades = Arnold Schwarzenegger, action of item 2: ace of hearts = screaming at, and object of item 3: two of diamonds = basketball) that can be decoded to retrieve items (Figure 1a for an example of compression system for cards used by the 6-time US Memory Champion)[20].

While we understand the techniques that memory athletes use, brain mechanisms behind their seemingly superhuman performance remain elusive. Prior neuroimaging studies of memory athletes averaged individual specificities across the group of memory athletes, an approach that has been shown to obscure details of functional brain organization[21,22]. Since each memory athlete trains slightly different techniques, the group level approach is also likely to average across inter-individual training-related differences. Group-averaged studies of memory athletes reported reduced fronto-parietal activity[23] potentially due to training effects[24], but also reported inconsistent

observations in retrosplenial cortex with either increased or decreased activity[25,26]. Differences between memory athletes and controls in resting-state functional connectivity (FC) were reported between memory and visual networks and, in the subcortex[27]. FC between the right anterior hippocampus and right caudate have also been found to correlate with memory athletes' world rankings[28].

We hypothesized that if a Memory Champion is consistently using his brain in unusual ways, such as cooperative processing between brain regions or networks that do not work together in most people, it would induce Hebbian plasticity[29]. This repeated processing between brain regions could lead to increased functional connectivity between them, observable during the resting state, and potentially leading to new functional modules[30]. We therefore tested for the presence of abnormally high cross-network resting-state FC, as indexed by network degree centrality[31], in a memory champion's brain.

To define individual-specific brain organization, we used a dense sampling approach, called precision functional mapping (PFM)[21,32] in which large amounts of highest-quality data are acquired for individual-specific analyses[33,34]. PFM has been used to successfully characterize longitudinal brain changes during pregnancy (n = 1)[34], to define cortical and subcortical network organization[11,21,35–37], to uncover novel networks (i.e., somato-cognitive action network (SCAN))[38,39], and to determine how they are shaped by plasticity[33,40]. In clinical populations, PFM has been used to identify a promising biomarker of depression[41], to characterize functional remapping following stroke[42], and to guide neuromodulation therapies[43].

For this study, we repeatedly scanned the 6-time US Memory Champion (in 2021 and 2015) obtaining >400 minutes of resting-state and >350 minutes of task fMRI data. In 2015, he performed the Midnight Scan Club (MSC) protocol[11], and we used the 10 MSC participants as controls. In 2021, he performed a tailored protocol to map neural circuits underlying his elite memory performance, and two of the MSC participants completed the same protocol as controls (see Table 1 for the list of tasks). We further compared the Memory Champion's brain, to a large adult population (n = 887 participants, 22-35 years old, Human Connectome Project (HCP))[44] to validate the specificity of his brain functional organization in addition to the 10 MSC participants.

Functional connectivity specific to the Memory Champion

Following the Hebbian plasticity hypothesis that training might strengthen functional connections, we aimed to identify regions in the Memory Champion's brain that showed stronger FC at rest. Thus, we compared his resting state FC maps to those of 887 individuals (aged 22-35) from the Human Connectome Project (HCP). For this comparison, we used 17 canonical functional networks (shown in Figure S1a; see the specificity analysis in Methods).

For each network we identified brain regions where the Memory Champion's functional connectivity was stronger than 95% of the controls. Several brain regions exhibited greater FC compared to controls with six or more functional networks at both timepoints (2015 and 2021 visits), indicating an elevated centrality of these regions compared to the general population (Figure 1c; Table E1).

Cortical regions with the highest centrality in the Memory Champion relative to controls included retrosplenial (context-association network), parieto-occipital (higher-order lateral visual), and frontal regions belonging to the language network, particularly those previously associated with semantic processing[45] (including Brodmann area 55b). In the Memory Champion's subcortex,

regions with the greatest centrality increases relative to controls were anterior caudate and central cerebellum. The caudate showed stronger FC with memory and executive networks (PMN, DMN, CAN, fronto-parietal network (FPN), Salience). In contrast, all cortical and the cerebellar high centrality regions showed greater FC mainly with visual and motor control networks (Table E1).

The same analyses performed on two matched controls (MSC02, MSC06), failed to reveal strong divergence from the HCP group data. Moreover, the regions with the relatively greatest differences from the HCP group data in the controls (MSC02, 06) did not overlap with the increased centrality regions in the Memory Champion (Figure S2). Further, no brain region in these controls showed stronger functional connectivity with more than 3 networks.

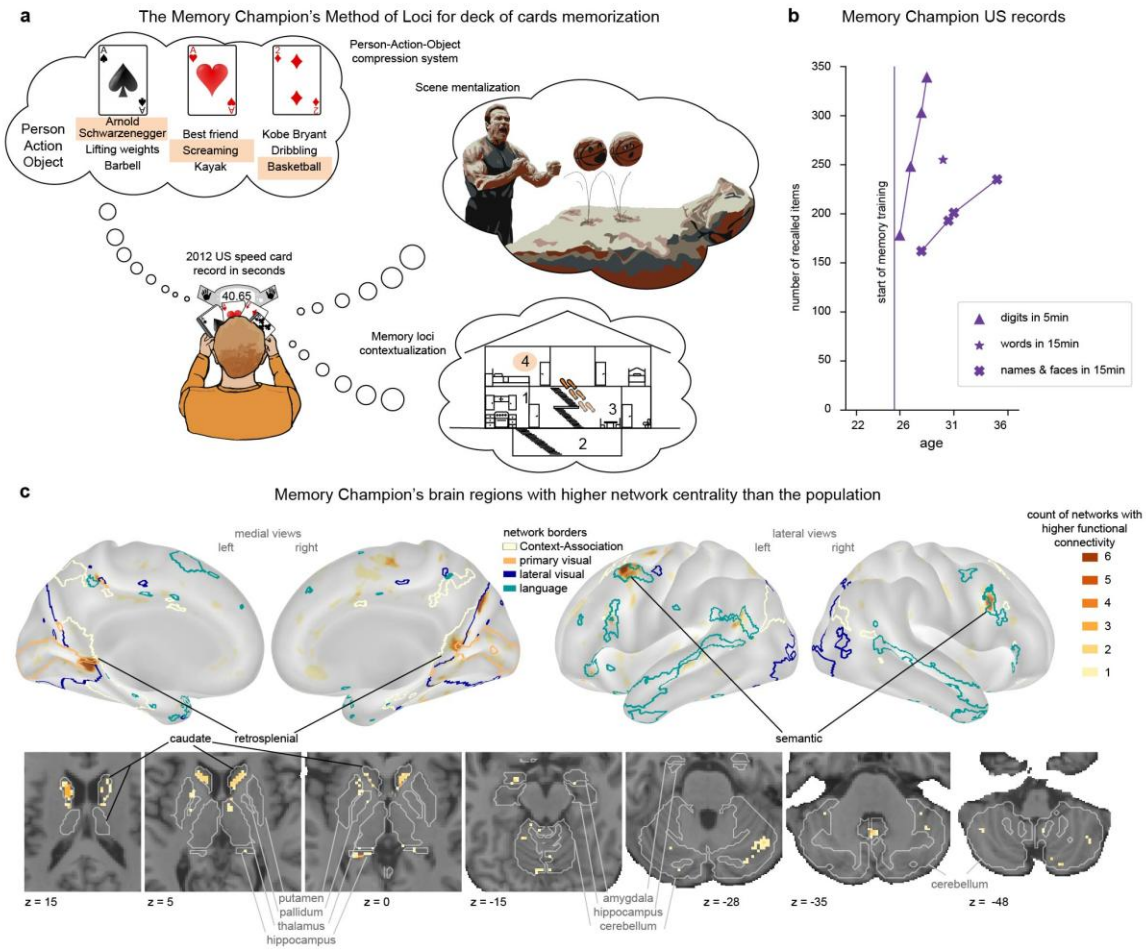

Figure 1: Brain of a memory champion: Memorization technique, performance and functional connectivity *a) Deck of card memorization strategy used by the 6x US Memory Champion. The strategy involves a pre-encoded association system where each card is linked to three items (person, action, object), combined into a scene ('Arnold Schwarzenegger (ace of spades) screaming at (ace of hearts) basketballs (two of diamonds)') represented at a specific location within one of the Memory Champion's memory palace loci, e.g. the bedroom of his house. b) 6x US Memory Champion's US records over the years. The number of recalled items for three official US records: digits in 5 minutes, words in 15 minutes, and names and faces in 15 minutes plotted as a function of his age. c) Memory Champion's brain regions with higher network centrality than the population. Regions with higher functional connectivity in the Memory Champion than 95% of individuals from the HCP population, at both visits (2015, 2021), with one or more of the 17 functional networks (see Figure S1a) after mixture modeling normalization of each network FC map (see*

Methods). Darker brown colors indicate stronger FC with a higher number of functional networks (from 1 to 6), indicating higher centrality. Boundaries for the language (teal), lateral visual (dark blue), primary visual (ochre), and context-association (CAN, white) network are shown in color.

Functional connectivity of high centrality regions

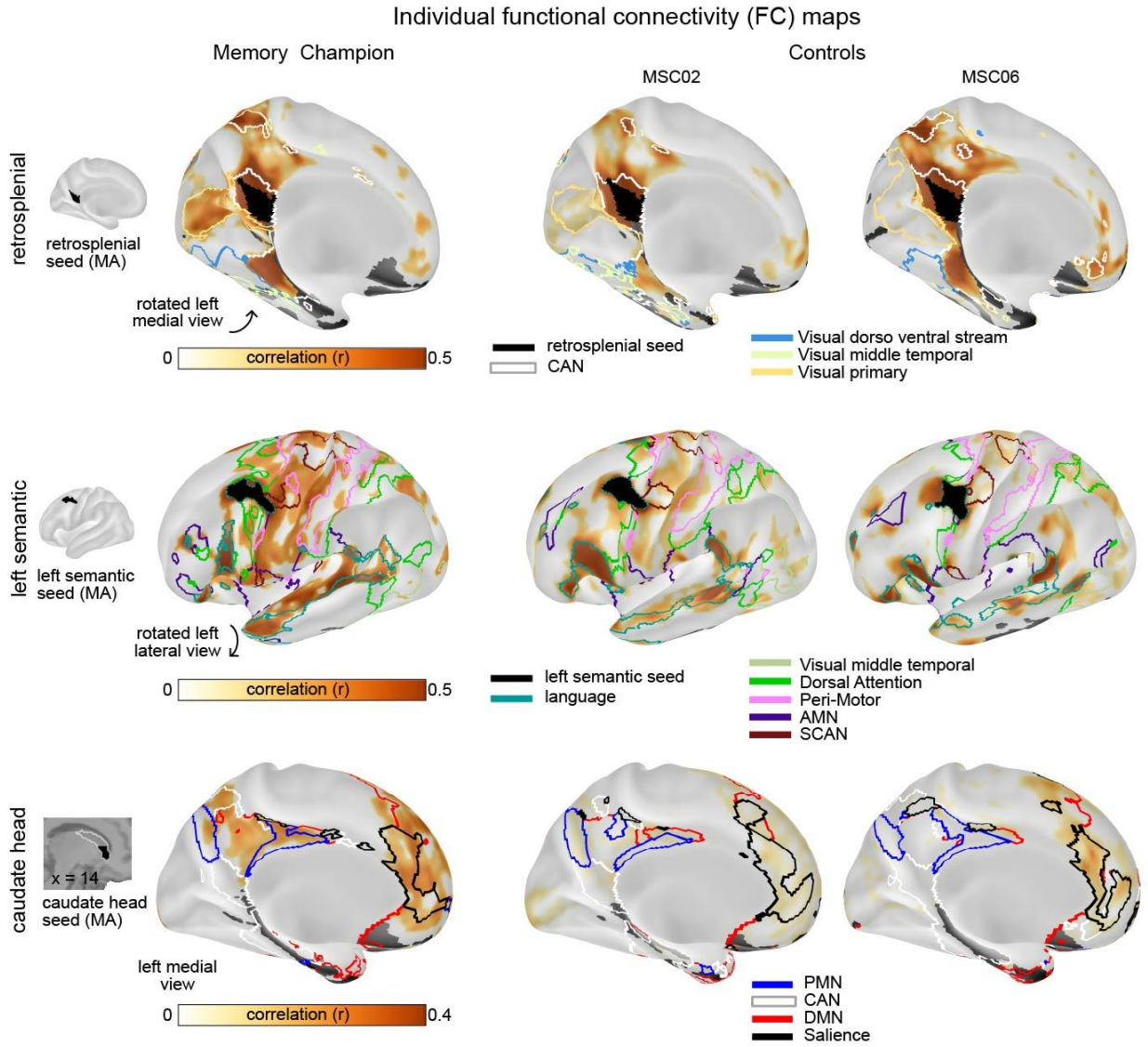

Figure 2: Functional connectivity of regions with high centrality in the Memory Champion. *Whole-brain FC maps for representative brain regions identified in Fig. 1c, top 20% of strongest connections are shown. Left column shows the memory champion, middle column MSC02 control, and right column MSC06 control (2021 data; see figure E2 for 2015 data, and figure S3 for additional brain views). The top row shows correlation (r) for retrosplenial cortex (Brodmann areas 26, 29, and 30, part of context-association network -white border), middle row shows the left semantic region (area 55b; language network -teal border) and the bottom row shows the head of the left caudate. The seed regions are shown in black. All other network borders indicate networks significantly more connected in the Memory Champion compared to the controls in 2021 (see Figure E2 for quantification). Network abbreviations: action-mode (AMN), somato-cognitive action (SCAN), parietal memory (PMN), context-association (CAN) and default mode (DMN). Low signal-to-noise masked areas are displayed in grey.*

To visualize the details of functional connectivity differences between the Memory Champion and matched repeatedly sampled controls (Figure 2 for the 2021 visit, see figure E2 for the 2015 data and figure S3 for additional brain views), we computed correlation maps for regions with the greatest centrality increases in the Memory Champion. We selected matching regions comparable between the Memory Champion and control participants: retrosplenial cortex (Brodmann areas 26, 29, and 30[9,46]), a left semantic region based on individual language network functional segmentation (see Figure E1, see Methods), and the head of the caudate (from individual anatomical segmentation, see Methods). Individual-specific seed maps were generated for each of these regions for the Memory Champion (Figure 2, left) and the two repeatedly sampled controls (Figure 2, middle & right; see Figure E2 for quantification of individual resting state scan distribution and t-test between Memory Athlete and PFM controls, $p<0.05$ after FDR).

The retrosplenial region showed significantly greater FC with visual networks in the Memory Champion compared to controls, particularly with the primary visual and dorso-ventral stream networks (Figure 2 top row). The left semantic region had significantly greater FC than controls with a set of networks involved in motion and action (Figure 2 middle row), namely the visual medial temporal network, which includes visual area 5 associated with motion perception[47], the dorsal attention network (associated with action imagery, figure S16), and the peri-motor, action-mode, and somato-cognitive action networks[48]. In the Memory Champion, the caudate head showed significantly stronger FC with memory networks (Parietal memory and context association networks) and the Salience network (Figure 2 bottom row). Stronger FC with the default mode network was only significant in the 2021 dataset. We also validated that similar results were observed when testing exploratively across all networks (Figure E2c).

Functional modules specific to the Memory Champion

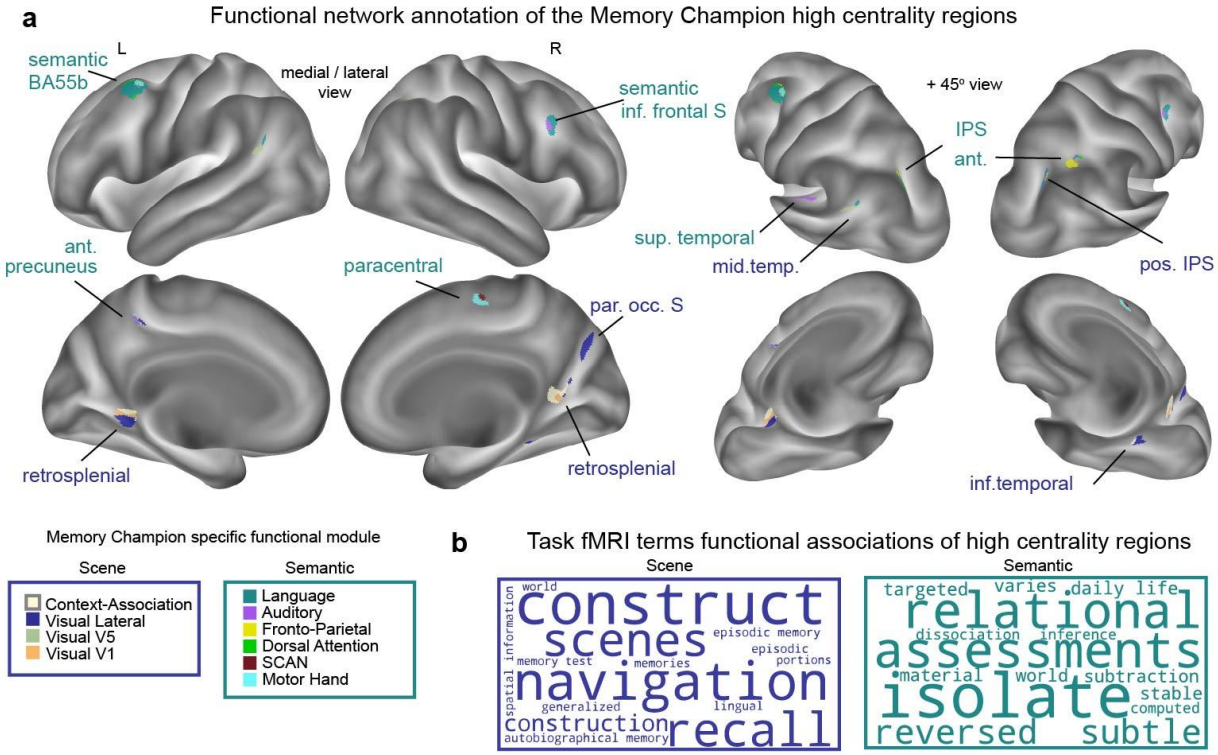

Figure 3: Functional modules only found in the Memory Champion. *a) Functional network annotation of the Memory Champion's high centrality regions. The memory champion's individual network labels, masked by high centrality regions from Figure 1c, are shown on an inflated brain. Regions are grouped into two sets of networks (network color label, bottom left) representing a scene (dark blue) and semantic (teal) module. Each region is named anatomically or functionally in dark blue for the scene module and teal for the semantic module. Abbreviations: parietal occipital sulcus (Par. Occ. S), intra parietal sulcus (IPS), somato-cognitive action network (SCAN), Brodmann Area (Ba). b) Top 15 Neurosynth terms associated with the Memory Champion's high centrality regions. Wordclouds of the terms most strongly associated with the Memory Champion's high centrality regions. The font size of the word matches the relative weight of the term amongst the top 15.*

To further characterize the function of the high centrality regions (Figure 3a), we annotated them based on their functional network labels. We named 'module' a group of regions showing functional similarities. One module belonged to the visual and context association networks, including the retrosplenial cortex, parietal occipital sulcus, middle and inferior temporal regions, and posterior intraparietal sulcus. The other module was part of language, auditory, executive (fronto-parietal and dorsal attention), and motor (somato-cognitive action and motor hand) networks, which included frontal regions from semantic part of the language network, anterior precuneus, paracentral lobule, superior temporal regions, and anterior intraparietal sulcus (see Table E1 for coordinates).

To investigate what is known about the high centrality regions of the Memory Champion, we annotated them using the automated meta-analytic Neurosynth term maps[49], which are based on activation peak coordinates from a large corpus of task fMRI studies (Figure 3b for module-level analysis and Figure E3 for replication at the individual region level). The set of high centrality regions contained in visual and context association networks were associated with terms related to scene representation: construct, navigation, scene, and recall. Therefore, we named this set of regions the 'scene module'. The other set of high centrality regions was associated with terms about abstract concept manipulation: isolate, assessment, relational, and reversed. Since the set of terms refers to abstract, analytic, or experiential concepts that are generally higher-level rather than sensory or formal, and several of these regions are within the semantic part of the language network, we can best summarize this module as the 'semantic module.'

The scene and semantic modules specific to the Memory Champion also emerged from the data when using other analytic approaches, such as principal component analysis on high centrality region FC maps, testing the functional similarity of high centrality regions against null hypotheses, and exploring module differences in network connectivity (see Module Analysis, Methods; Figure E4).

Expanded memory networks in the caudate

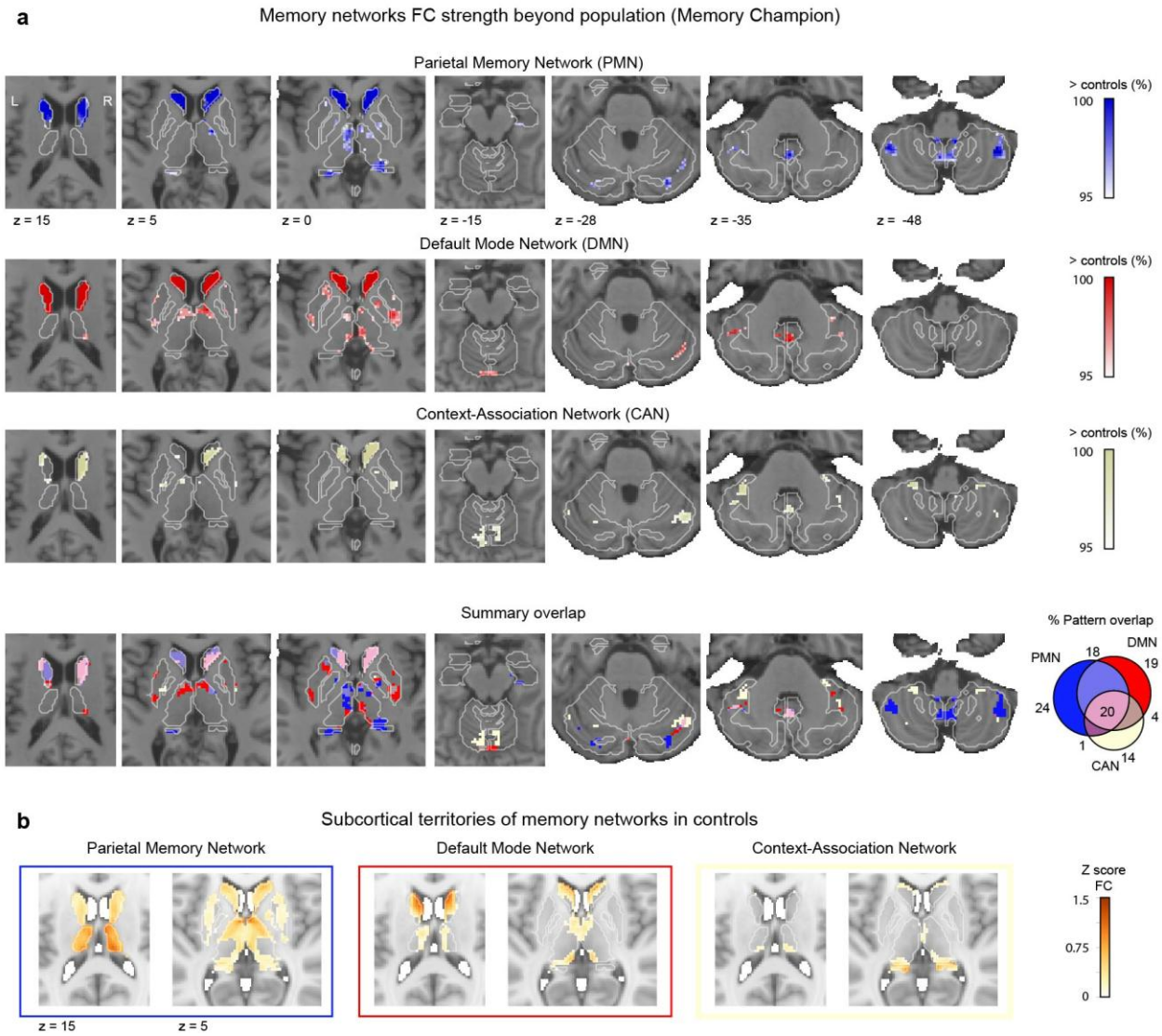

Figure 4: Subcortex to memory networks functional connectivity. *a) Subcortical regions where the Memory Champion showed stronger FC than 95% of controls (HCP), by network: top row Parietal-Memory network (PMN, blue), second row Default-Mode network (DMN, red) and third row Context-Association network (CAN, white) FC maps in subcortex. The overlap across networks is shown in the fourth row, with pink indicating greater functional connectivity to all three memory networks. Results are displayed on the Memory Champion's horizontal T1 structural slices with the network labelled color as gradient scale (right). White borders outline the Freesurfer segmented anatomical structures. See Figure E5 and S13 for replication in 2015 data. b) Subcortical functional connectivity of memory networks in controls (HCP). Left to right, PMN (blue), DMN (red), CAN (white) Z scored FC maps for regions where networks are competing for winner-take-all labels. Results are displayed on the MNI horizontal T1 structural slices. White borders outline anatomical structures. (See Figure E6 for winner take all maps, figure E7 for more subcortical slices of control network territories and a quantification of the overlap with the Memory Champion's Memory network high centrality from panel a. See Figure S14 for subcortical network territories of the Memory Champion).*

To further analyze the Memory Champion's high centrality regions in subcortex, we mapped out voxels where his FC was stronger than 95% of the controls (HCP), for each of the memory

networks (DMN, PMN, CAN) (Figure 4a; 2015 replication in Figure S13). The Memory Champion had stronger FC between the striatum and all memory networks, particularly in the caudate (FC > 100% of controls). Mapping voxels with the stronger FC across the memory networks revealed a substantial overlap in the head of the caudate (Figure 4a; replication with 2015 data in Figure E5).

In addition to generally stronger connectivity to the striatum, we found that the Memory Champion had a pattern of subcortical functional connectivity in relation to memory systems that was distinct from controls. Specifically, whereas controls only exhibited FC between caudate and the PMN and DMN, the Memory Champion additionally demonstrated substantial connectivity to the CAN (See Figure 4a third raw and Figure 4b third column). This difference is quantified in Figure E7 by testing the significance of the percent overlap of the stronger subcortical connectivity within the memory networks of the Memory Champion compared to each network subcortical territory in the controls (regions showing strong network connectivity and candidates for the winner-take-all labeling; see Methods). This suggests that the Memory Champion has strengthened existing functional connections and also possesses some connectivity absent in controls (CAN).

Comparing rote memorization and Method of Loci

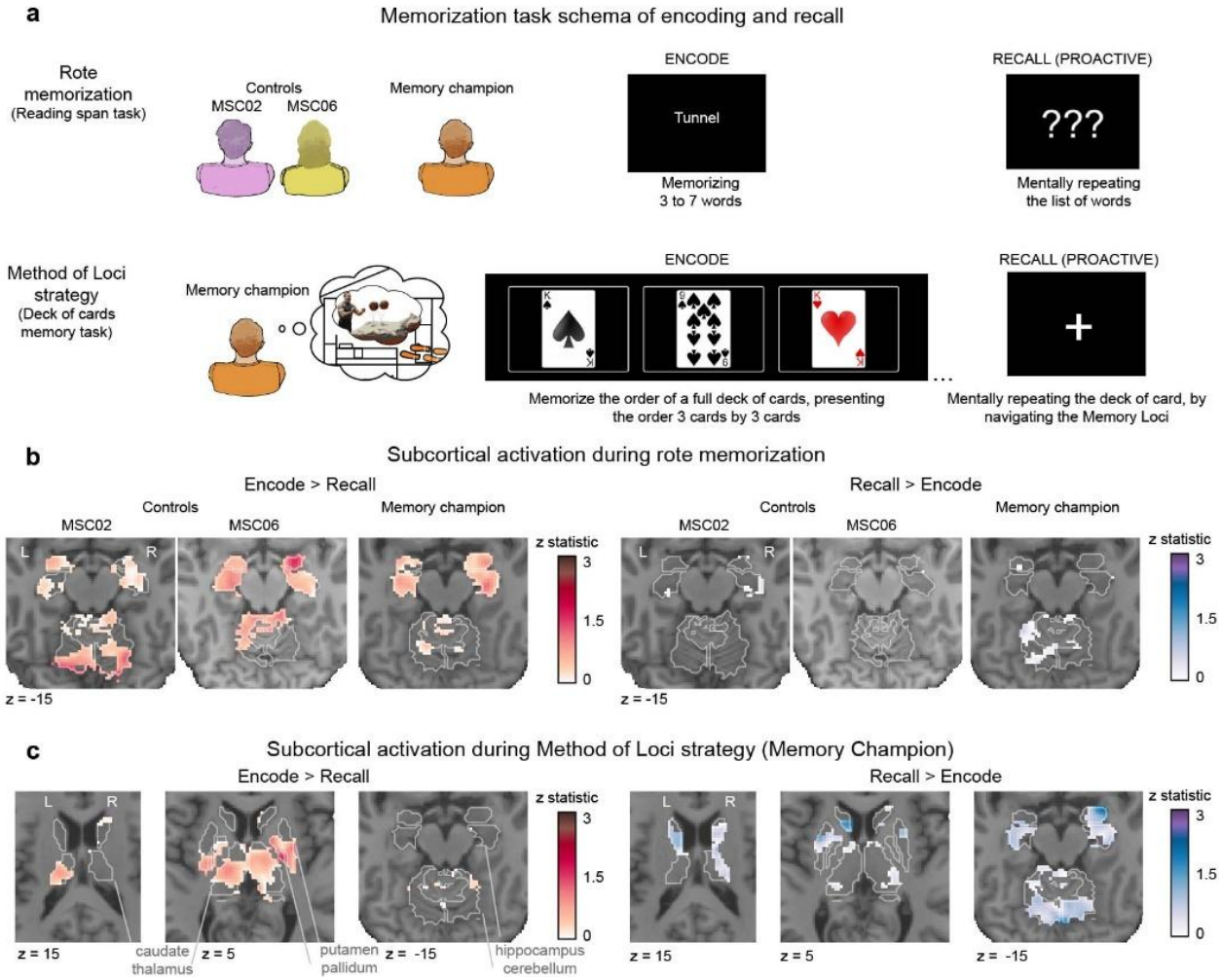

Figure 5: Task activations during encoding and recall when using rote memorization or Method of Loci. *a) Reading span and Deck of cards memory task schemas for encoding and recall (proactive).*

Schema shows the encoding and proactive recall phases of the reading span task (top line) and the Deck of cards memory task (bottom line). Full task schemes are available in figures S18 and S20. b) Task fMRI contrast of Encoding versus Recall, when using rote memorization in the Reading span task. Results are shown on each participant T1 horizontal slice (z = -15) for unthresholded Z-statistic maps of Encode > Recall (left) and Recall > Encode (right), for controls (MSC02, MSC06) and the Memory Champion (2021 data). White borders outline anatomical structures (Freesurfer segmentation). For additional slices and cortical results see figure E8. c) Task fMRI activation of Encode versus Recall contrasts when the Memory Champion is using the Method of Loci strategy in the Deck of cards task. Controls are unable to perform this task. Results are shown on the Memory Champion's T1 horizontal slices (z = 15, 5, -15) for unthresholded Z-statistic maps of Encode > Recall (left) and Recall > Encode (right), with white borders of anatomical structures. For cortical results see figure E9.

To understand whether the Memory Champion's high centrality regions are related to his memory performance, we analyzed task fMRI activity during the performance of two memory tasks. One task was a working memory Reading span task performed by controls and the Memory Champion, for which the Memory Champion was instructed not to use any memory techniques. Participants engaged in rote rehearsal of the items (3 to 7 words, encoding) before being cued to silently recall them (proactive recall) (Figure 5a).

The second task was a tailor-made task that only the Memory Champion could perform, in which he used the Method of Loci and the Person-Action-Object compression system (Figure 1a) to memorize the order of a deck of cards (Deck of cards memory task, Method; Figure 5a). The encoding phase, during which the deck was displayed 3 cards at a time, was followed by a proactive recall phase, in which the Memory Champion retrieved the order of the deck of cards just memorized by navigating his memory loci. Correct memorization of the deck order was tested outside of the scanner. We compared encoding and recall neural activity in both tasks to capture the neural circuit underlying his superior memory performance.

During rote memorization (Figure 5b) controls (MSC02 and MSC06) and the Memory Champion showed similar activations in subcortex (Figure 5b) and cortex (Figure E8). This pattern of activation was consistent with previously published work[50,51], including larger activation of the DMN in encoding and PMN in recall. Rote memorization elicited more hippocampal activity during encoding than proactive recall, again consistent with previously published work[52].

In sharp contrast, when using the Method of Loci, the Memory Champion showed the reverse pattern, with greater hippocampal activity during recall than encoding (Figure 5c). Cortical activations were also very different between the two strategies (Figure E9 and S15), including frontal regions consistent with strategy based memorization[53]. Both encoding and proactive recall elicited activity in specific parts of the caudate during Method of Loci memorization, highlighting the overall importance of the caudate in this mnemonic strategy. Notably, average activation evoked in the high-centrality regions identified by FC was greater for Method of Loci compared to rote memorization in encoding versus recall contrasts (Figure S17).

High centrality regions during Method of Loci training

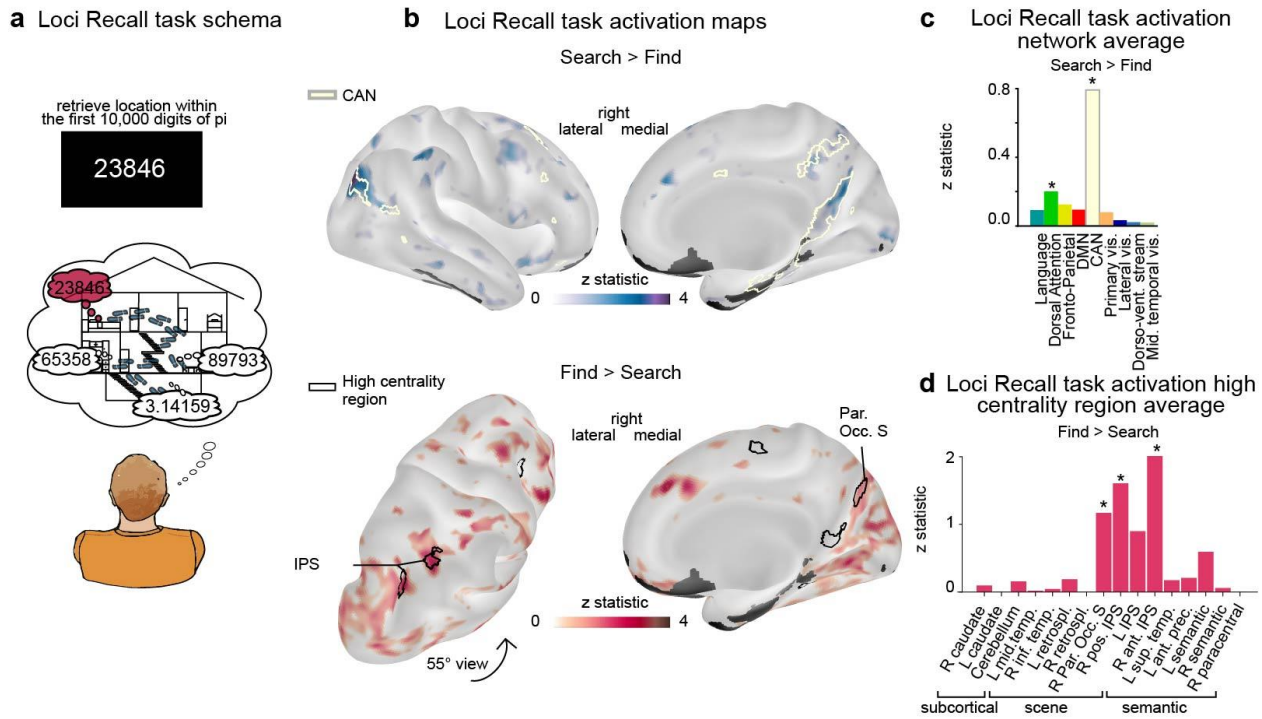

Figure 6: Task fMRI activation when recalling digits of the number pi using Method of Loci. *a) task schema of a locus recall trial within the number of pi task. Mental navigation (search in blue) and retrieval (found in red) of the locus where a prompted unique 5-digits sequence from the pre-learned 10,000 first digits of the number of pi is stored. Contrasted events are 'search' (failed to find within 6 seconds) and 'found' (localized within 6 seconds) events. (see Figure S19 for full task schema) b) Cortical activation during recall of 5-digits sequence location within the 10,000 first digits of the number of pi by the Memory Champion contrasting search only (loci navigation) and finding (search and localization). Inflated right lateral and medial views of the positive Z-statistic cortical maps of Search > Found (top) and Found > Search (bottom). Context association network (CAN) borders (white outlines) are displayed on Search > Found views and the memory champion high centrality region borders (black outlines) are displayed on Found > Search c) Network average Z-statistic bar plot for Search > Found. d) Average Z statistics per high centrality regions grouped by subcortical regions and scene and semantic modules. (*, P < 0.05, FDR). Low signal-to-noise masked areas are displayed in grey.*

To better understand whether the Memory Champion's high centrality regions are related to his memory training, we designed a task based on a memory challenge he was preparing for at the time: fast retrieval of the locations of 5-digit sequences within the first 10,000 digits of pi. Having already memorized the first 10,000 digits of pi, he was presented with a series of 5-digit sequences and asked to retrieve their locations within the overall sequence of pi. We contrasted the neural activation during failed trials (search only) and successful trials (search + found) (Figure 6). The search process significantly activated the dorsal attention network and an extended portion of the CAN. Finding the location of the 5-digit sequence was associated with greater activation of the visual cortex and showed significant activation of several high centrality regions (IPS, Figure 6b bottom), including the parietal occipital sulcus and the intraparietal sulcus regions. These results indicate that the Memory Champion's practice methods engage

some of the same brain regions that exhibited altered functional connectivity (higher centrality relative to controls) in the resting state.

Alternative circuits for memory

Elite memory abilities built are on intense training, leading to unique skillset. Method of Loci strategies are supported by a fundamentally different set of cortical and subcortical regions compared to rote memorization (Figures 5 and E8) that might benefit from differences in goals or strategies[54] and the types of information being encoded[55]. Method of Loci memorization and recall seem to depend on the caudate, which is involved in rule-based learning[15], and unique modules involved in scene representation, and semantic concept manipulation (Figure 3). Notably, the hippocampus is most active during Method of Loci recall, not encoding. The level of activation of the hippocampus during encoding paired items typically predicts success in recall[56–58]. However, when using his overtrained Method of Loci strategies, the Memory Champion hippocampal activity is less than during encoding than recall, suggesting that little effort may be required on his part despite the nominal complexity of his strategy. In contrast, when using rote memorization, the Memory Champion showed the same activity patterns as controls, relying on classical memory networks (DMN[4], PMN[5,6]), for encoding and recollection (Figure E8 and S17). In both the Memory Champion and controls, the hippocampus was most active during rote encoding, eliminating the idea that his hippocampus may somehow be generally “overtrained”.

It is perhaps unsurprising that human brains can solve a basic problem, such as remembering the sequence of abstract pieces of information, in multiple ways. Yet, it is startling that colossal improvements in memorization capacity and speed can be unlocked by using strategies that recruit specific memory machinery to circumvent memory limitations by concretizing items to memorize. It seems that human memory systems specialized for spatial navigation, and social cognition, such as recording scenes involving other humans and skill learning, have capacities that can be co-opted by practicing specific techniques.

Speed through the caudate

The caudate is crucial for motor learning, skill acquisition, and habit formation. The caudate is primarily involved in associative learning, such as stimulus-response, rule-based strategies, or category learning[15]. It is also involved in spatial navigation, specifically egocentric navigation using self-reference[59], used in the Method of Loci. The caudate is thought to use fast plasticity to store details, in single-shot learning important for episodic memory[7,60], specially to link information together. In contrast, neocortical learning, and schema development supported by the anterior hippocampus, are thought to be slower in encoding information for generalization and semantic knowledge acquisition. Both circuits show an antagonistic relationship in which activation in the anterior hippocampus decreased, whereas caudate activity increased[61] and in which rule-based approaches are favored when available[62], which may partially account for the observed lower activity of the hippocampus during Method of Loci encoding compared to recall (Figure 5c).

During stimulus-response learning, activation has been observed in the head of the caudate, progressing toward the tail with increased learning performance[62], and the tail potentially coding for confidence value[63]. As part of the dopamine system, which promotes plasticity through reward prediction error[60], the caudate might play a specific role in evaluating confidence value during learning[64], potentially producing internal feedback using a rule-based model[60] to predict a response and compare it to the stored detailed information. The predictive role of the caudate could also be functionally significant in simulating the memory loci themselves, and which details

are associated to each locus during mental spatial navigation, associative learning and retrieval within the Method of Loci (Figure 5c). This co-localization of fast memorization, action circuitry and navigation could have an evolutionary importance, supporting archaeological evidence for heightened mobility and spatially extensive social networks of modern human compared to Neandertal[65].

Context and narration enhance memory span

Brain activity elicited by the Method of Loci was greater in the visual and context-association networks when the Memory Champion encoded information versus recalling it (Figure E9), consistent with his strategy premised on scenes building and visualization with persons, actions, and objects in a specific mental location. The retrosplenial cortex active during search of items through the Loci (Figure 6) was also active during the place localizer task (Figure S16), highlighting a role in spatial information processing, consistent with is known role in spatial contextualization[8,66]. The broad activation of visual regions coincides with Memory Champion reported use of concrete imagery in his rapid encoding, suggesting that he actively represents the scene of elements associated with abstract concepts (such as cards (see similarities in his brain activation during cards and elements viewing in Figure S16) or digits) that he aims to encode, leveraging the scene representation module (Figures E9 and 6c).

The brain regions constituting the semantic module showed increased centrality with action networks (Table E1). Particularly the left semantic region, which includes Brodmann area 55b, is one of the language regions that develop later in children[67], known to be active in story listening[68], specifically processing information related to syntax and story event boundaries[69]. We hypothesized that the semantic module is involved in tracking the sequence of actions within the narrative building across memory loci. As the Memory Champion explains, *"a true, powerful, memorable mental image needs to be created with all of the senses, not just mental sight. […] Lastly, […] add movement…. For whatever reason, things that move are difficult to forget. My theory is that by making it move, you've suddenly made that still photo in your mind an actual story"*[17]. Prior to the invention of writing systems, complex histories would be transmitted as stories and songs. Homer's Odyssey was passed along orally from memory, prior to being written down, providing ancient evidence for superior story encoding and recall spans[70]. Evidence of large knowledge memorization relating ancient historical events was also demonstrated in oral culture of Australian Aboriginal community[71], suggesting deliberate use of narration for its superior memorizability[72]. In other words, a key component of the superior abilities of memory athletes may be their capacity to convert arbitrary information into easily imageable scenes[73] that help create a highly memorable narrative structure[74].

Module based enhanced cognition

It remains possible that the Memory Champion and other memory athletes were born with an innate talent for memorization, despite our Memory Champion's self-reports to the contrary[17]. However, the activity of the semantic and scene modules (Figure 6c), and the improvement in his performance over the years (Figure 1b), suggest that the specific patterns of connectivity in his brain may have been shaped by memory training through repeated co-activation. Indeed, as the Memory Champion wrote: *"After years of using these techniques, my images boil down to a nuance that I can't explain in writing. It's almost like a feeling"*[20]. Together with the late maturation of Brodmann area 55b[67], these regions may flexibly combine into processing modules that support strategies which enhance cognition. Thus, specific mnemonic strategies like the Method of Loci may significantly improve learning and memory capabilities much like neural plasticity in other

brain regions observed in the formation of reading[75] and writing abilities[76]. These findings hint at a general ability of the brain to acquire new skills via flexibly connecting regions into novel modules, that add additional organization, without harm to existing abilities. From our knowledge of the brain, one could imagine other cognitive strategies that focus on leveraging existing neural circuits that are able to overcome the limitations of the default circuitry.

Circuits preserved in aging

The Memory Champion's functional regional specialization through training provides ideas on how to enhance cognitive resilience in aging. Mnemonic techniques, particularly the Method of Loci, seem to leverage skills such as egocentric navigation and tracking event boundaries in stories, that are relatively more preserved in healthy aging[69,77]. The Method of Loci has shown promise in the aging population, with individuals able to achieve high memory performance using the technique and remaining proficient with it at six-year follow-up[78]. Major changes in routine and relocation can bring stress and anxiety to some older adults, linked to difficulty adapting and acquiring new landmarks[79,80]. Moreover, the context-association network has been shown to be a mediator between the Default Mode Network (DMN) and the hippocampus, with amplitude of the CAN to medial temporal lobe functional connectivity associated with better episodic memory performance in older adults[9]. This suggests the possibility that robust CAN function might support stable memory function during aging. Thus, exploring the use of the Method of Loci to reinforce CAN functioning is an exciting prospect for maintaining cognitive abilities and fostering a resilient brain.

Making 'memory' memorable

The wide gulf between our ability to remember random sequences of abstract symbols and our ability to navigate without getting lost, or to remember salient social interactions, hints at the skills that mattered most across our evolutionary history[65]. While able to accomplish complex cognitive tasks that still elude artificial intelligence, it is surprising that human general-purpose memory for abstract symbols is so limited and so easily implemented by computers. Our memories might have evolved for human-specific tasks, including navigation and storytelling[81]. As it turns out, the best memory is goal oriented. In the age of supercomputers and AI, human rote memorization is already near-obsolete. Thus, it might be a great time to make teaching, learning and working more naturally human friendly, by leaning into our strengths. While computer memory and AI are beating expert humans at most things, we still have much to discover about our own abilities as still unbeaten mobile, social, energy efficient entities[82,83].

Acknowledgement

We would like to extend our sincere gratitude to Nelson Dellis for his invaluable contribution and participation in this study. This work was supported by NIH grants NS140256 (E.M.G.), NS123345 , NS098482 (B.P.K.),MH129616 (T.O.L.), T32DA007261 (S.R.K), MH096773 (N.U.F.D.), MH122066 (N.U.F.D., E.M.G.), MH121276 (N.U.F.D. , E.M.G.), MH124567 (N.U.F.D. , E.M.G.), NS129521 (N.U.F.D. , E.M.G.), and NS088590 (N.U.F.D.); by the Taylor Family Foundation (T.O.L.); by the Intellectual and Developmental Disabilities Research Center (N.U.F.D.); by the Kiwanis Foundation (N.U.F.D.); by the Washington University Hope Center for Neurological Disorders (B.P.K. and N.U.F.D.); by Mallinckrodt Institute of Radiology pilot funding (N.U.F.D.); by the McDonnell Center for Systems Neuroscience and the Brain and Behavior Research Foundation (R.J.C.) . Computations were performed using the facilities of

the Washington University Research Computing and Informatics Facility, which were partially funded by NIH grants S10OD025200, 1S10RR022984-01A1 and 1S10OD018091-01.

Conflict of Interest

E.M.G. may receive royalty income based on technology developed at Washington University School of Medicine and licensed to Turing Medical Inc. N.U.F.D. has a financial interest in Turing Medical Inc. and may benefit financially if the company is successful in marketing Framewise Integrated Real-Time Motion Monitoring (FIRMM) software products. N.U.F.D. may receive royalty income based on FIRMM technology developed at Washington University School of Medicine and Oregon Health and Sciences University and licensed to Turing Medical Inc. N.U.F.D. is a co-founder of Turing Medical Inc. TOL is a consultant for Turing Medical Inc. TOL holds a patent for taskless mapping of brain activity licensed to Sora Neurosciences and a patent for optimizing targets for neuromodulation, implant localization, and ablation is pending. These potential conflicts of interest have been reviewed and are managed by Washington University School of Medicine. The other authors declare that they have no known competing financial interests or personal relationships that could have appeared to influence the work reported in this paper.

Reference

1. Forsberg, A., Adams, E. J. & Cowan, N. Chapter One - The role of working memory in long-term learning: Implications for childhood development. in *Psychology of Learning and Motivation* (ed. Federmeier, K. D.) vol. 74 1–45 (Academic Press, 2021).
2. Rolls, E. T. & Treves, A. A theory of hippocampal function: New developments. *Progress in Neurobiology* **238**, 102636 (2024).
3. Henke, K. A model for memory systems based on processing modes rather than consciousness. *Nat Rev Neurosci* **11**, 523–532 (2010).
4. Raichle, M. E. The brain's default mode network. *Annu Rev Neurosci* **38**, 433–447 (2015).
5. Gilmore, A. W., Kalinowski, S. E., Milleville, S. C., Gotts, S. J. & Martin, A. Identifying task-general effects of stimulus familiarity in the parietal memory network. *Neuropsychologia* **124**, 31–43 (2019).
6. Wei, X. & Buckner, R. L. Old-New Recognition Memory Revisited. 2025.11.11.687844 Preprint at https://doi.org/10.1101/2025.11.11.687844 (2025).
7. Buzsáki, G. & Moser, E. I. Memory, navigation and theta rhythm in the hippocampal-entorhinal system. *Nat Neurosci* **16**, 130–138 (2013).

8. Czajkowski, R. *et al.* Encoding and storage of spatial information in the retrosplenial cortex. *Proceedings of the National Academy of Sciences* **111**, 8661–8666 (2014).

9. Kaboodvand, N., Bäckman, L., Nyberg, L. & Salami, A. The retrosplenial cortex: A memory gateway between the cortical default mode network and the medial temporal lobe. *Hum Brain Mapp* **39**, 2020–2034 (2018).

10. Aminoff, E. M., Kveraga, K. & Bar, M. The role of the parahippocampal cortex in cognition. *Trends Cogn Sci* **17**, 379–390 (2013).

11. Gordon, E. M. *et al.* Precision Functional Mapping of Individual Human Brains. *Neuron* **95**, 791-807.e7 (2017).

12. Egner, T. The Caudate Nucleus Mediates Learning of Stimulus–Control State Associations. *J Neurosci* **37**, 1028–1038 (2017).

13. Kwon, Y. H. *et al.* Situating the salience and parietal memory networks in the context of multiple parallel distributed networks using precision functional mapping. *Cell Rep* **44**, 115207 (2025).

14. Wei, X. & Buckner, R. L. Old-New Recognition Memory Revisited. *bioRxiv* 2025.11.11.687844 (2025) doi:10.1101/2025.11.11.687844.

15. Seger, C. A. & Cincotta, C. M. The Roles of the Caudate Nucleus in Human Classification Learning. *J Neurosci* **25**, 2941–2951 (2005).

16. Oberauer, K., Farrell, S., Jarrold, C. & Lewandowsky, S. What limits working memory capacity? *Psychological Bulletin* **142**, 758–799 (2016).

17. Dellis, N. *Memory Superpowers!: An Adventurous Guide to Remembering What You Don't Want To Forget*. (Abrams Books for Young Readers, 2020).

18. Hughes, J. E. A. *et al.* Savant syndrome has a distinct psychological profile in autism. *Molecular Autism* **9**, 53 (2018).

19. Roediger, H. L. The effectiveness of four mnemonics in ordering recall. *Journal of Experimental Psychology: Human Learning and Memory* **6**, 558–567 (1980).

20. Dellis, N. *Improve Your Memory: With the Astonishing Memory Palace Technique: Includes 52 Cards, 64-Page Book, and a Fold-Out Memory Map Poster*. (Arcturus Publishing, 2024).

21. Laumann, T. O. *et al.* Functional System and Areal Organization of a Highly Sampled Individual Human Brain. *Neuron* **87**, 657–670 (2015).

22. Gratton, C. *et al.* Functional Brain Networks Are Dominated by Stable Group and Individual Factors, Not Cognitive or Daily Variation. *Neuron* **98**, 439-452.e5 (2018).

23. Ren, J. *et al.* Method of loci training yields unique neural representations that support effective memory encoding. 2025.02.24.639840 Preprint at https://doi.org/10.1101/2025.02.24.639840 (2025).

24. D'Esposito, M. & Postle, B. R. The Cognitive Neuroscience of Working Memory. *Annual Review of Psychology* **66**, 115–142 (2015).

25. Wagner, I. C. *et al.* Durable memories and efficient neural coding through mnemonic training using the method of loci. *Sci Adv* **7**, eabc7606 (2021).

26. Maguire, E. A., Valentine, E. R., Wilding, J. M. & Kapur, N. Routes to remembering: the brains behind superior memory. *Nat Neurosci* **6**, 90–95 (2003).

27. Dresler, M. *et al.* Mnemonic Training Reshapes Brain Networks to Support Superior Memory. *Neuron* **93**, 1227-1235.e6 (2017).

28. Müller, N. C. J. *et al.* Hippocampal–caudate nucleus interactions support exceptional memory performance. *Brain Struct Funct* **223**, 1379–1389 (2018).

29. Fox, K. & Stryker, M. Integrating Hebbian and homeostatic plasticity: introduction. *Philosophical Transactions of the Royal Society B: Biological Sciences* **372**, 20160413 (2017).

30. Bassett, D. S. *et al.* Dynamic reconfiguration of human brain networks during learning. *Proceedings of the National Academy of Sciences* **108**, 7641–7646 (2011).

31. Rubinov, M. & Sporns, O. Complex network measures of brain connectivity: Uses and interpretations. *NeuroImage* **52**, 1059–1069 (2010).

32. Ooi, L. Q. R. *et al.* Longer scans boost prediction and cut costs in brain-wide association studies. *Nature* 1–10 (2025) doi:10.1038/s41586-025-09250-1.

33. Newbold, D. J. *et al.* Plasticity and Spontaneous Activity Pulses in Disused Human Brain Circuits. *Neuron* **107**, 580-589.e6 (2020).

34. Pritschet, L. *et al.* Neuroanatomical changes observed over the course of a human pregnancy. *Nat Neurosci* **27**, 2253–2260 (2024).

35. Krimmel, S. R. *et al.* The human brainstem's red nucleus was upgraded to support goal-directed action. *Nat Commun* **16**, 3398 (2025).

36. Marek, S. *et al.* Spatial and Temporal Organization of the Individual Human Cerebellum. *Neuron* **100**, 977-993.e7 (2018).

37. Badke D'Andrea, C. *et al.* Action-mode subnetworks for decision-making, action control, and feedback. *Proceedings of the National Academy of Sciences* **122**, e2502021122 (2025).

38. Gordon, E. M. *et al.* A somato-cognitive action network alternates with effector regions in motor cortex. *Nature* **617**, 351–359 (2023).

39. Braga, R. M. & Buckner, R. L. Parallel Interdigitated Distributed Networks within the Individual Estimated by Intrinsic Functional Connectivity. *Neuron* **95**, 457-471.e5 (2017).

40. Chauvin, R. J. *et al.* Disuse-driven plasticity in the human thalamus and putamen. *Cell Reports* **44**, 115570 (2025).

41. Lynch, C. J. *et al.* Expansion of a frontostriatal salience network in individuals with depression. 2023.08.09.551651 Preprint at https://doi.org/10.1101/2023.08.09.551651 (2023).

42. Laumann, T. O. *et al.* Brain network reorganisation in an adolescent after bilateral perinatal strokes. *The Lancet Neurology* **20**, 255–256 (2021).

43. Nahas, Z. *et al.* Personalized Adaptive Cortical Electro-stimulation (PACE) in Treatment-Resistant Depression. Preprint at https://doi.org/10.31234/osf.io/5c3ba_v1 (2025).

44. Van Essen, D. C. *et al.* The Human Connectome Project: A data acquisition perspective. *NeuroImage* **62**, 2222–2231 (2012).

45. Hodgson, V. J., Lambon Ralph, M. A. & Jackson, R. L. Multiple dimensions underlying the functional organization of the language network. *NeuroImage* **241**, 118444 (2021).

46. Vann, S. D., Aggleton, J. P. & Maguire, E. A. What does the retrosplenial cortex do? *Nat Rev Neurosci* **10**, 792–802 (2009).

47. Delikishkina, E., Lingnau, A. & Miceli, G. Neural correlates of object and action naming practice. *Cortex* **131**, 87–102 (2020).

48. Dosenbach, N. U. F., Raichle, M. & Gordon, E. M. The brain's cingulo-opercular action-mode network. https://doi.org/10.31234/osf.io/2vt79 (2024) doi:10.31234/osf.io/2vt79.

49. Yarkoni, T., Poldrack, R. A., Nichols, T. E., Van Essen, D. C. & Wager, T. D. Large-scale automated synthesis of human functional neuroimaging data. *Nat Methods* **8**, 665–670 (2011).

50. Thommesen, K. K. *et al.* Neural underpinnings of memory encoding and retrieval: Validation of a novel ecologically valid fMRI paradigm. *Neuroscience Applied* **3**, 104084 (2024).

51. Kim, H. Neural activity that predicts subsequent memory and forgetting: a meta-analysis of 74 fMRI studies. *Neuroimage* **54**, 2446–2461 (2011).

52. Grön, G. *et al.* Hippocampal Activations during Repetitive Learning and Recall of Geometric Patterns. *Learn Mem* **8**, 336–345 (2001).

53. Delazer, M. *et al.* Learning by strategies and learning by drill—evidence from an fMRI study. *NeuroImage* **25**, 838–849 (2005).

54. Otten, L. J. & Rugg, M. D. Task-dependency of the neural correlates of episodic encoding as measured by fMRI. *Cereb Cortex* **11**, 1150–1160 (2001).

55. Kelley, W. M. *et al.* Hemispheric specialization in human dorsal frontal cortex and medial temporal lobe for verbal and nonverbal memory encoding. *Neuron* **20**, 927–936 (1998).

56. Borders, A. A., Aly, M., Parks, C. M. & Yonelinas, A. P. The hippocampus is particularly important for building associations across stimulus domains. *Neuropsychologia* **99**, 335–342 (2017).

57. Meltzer, J. A. & Constable, R. T. Activation of human hippocampal formation reflects success in both encoding and cued recall of paired associates. *Neuroimage* **24**, 384–397 (2005).

58. Clark, I. A., Kim, M. & Maguire, E. A. Verbal Paired Associates and the Hippocampus: The Role of Scenes. *J Cogn Neurosci* **30**, 1821–1845 (2018).

59. Colombo, D. *et al.* Egocentric and allocentric spatial reference frames in aging: A systematic review. *Neuroscience & Biobehavioral Reviews* **80**, 605–621 (2017).

60. Seger, C. A. & Miller, E. K. Category Learning in the Brain. *Annual review of neuroscience* **33**, 203 (2010).

61. Poldrack, R. A. & Packard, M. G. Competition among multiple memory systems: converging evidence from animal and human brain studies. *Neuropsychologia* **41**, 245–251 (2003).

62. Seger, C. A. & Cincotta, C. M. Dynamics of Frontal, Striatal, and Hippocampal Systems during Rule Learning. *Cereb Cortex* **16**, 1546–1555 (2006).

63. Williams, Z. M. & Eskandar, E. N. Selective enhancement of associative learning by microstimulation of the anterior caudate. *Nat Neurosci* **9**, 562–568 (2006).

64. Scimeca, J. M. & Badre, D. Striatal contributions to declarative memory retrieval. *Neuron* **75**, 380–392 (2012).

65. Burke, A. Spatial abilities, cognition and the pattern of Neanderthal and modern human dispersals. *Quaternary International* **247**, 230–235 (2012).

66. Smallwood, J. *et al.* The default mode network in cognition: a topographical perspective. *Nat Rev Neurosci* **22**, 503–513 (2021).

67. Tu, J. C. *et al.* Commonality and Variability in Functional Networks In Young Children Under 5 Years Old. 2025.09.12.675913 Preprint at https://doi.org/10.1101/2025.09.12.675913 (2025).

68. Glasser, M. F. *et al.* A multi-modal parcellation of human cerebral cortex. *Nature* **536**, 171–178 (2016).

69. Reagh, Z. M., Delarazan, A. I., Garber, A. & Ranganath, C. Aging alters neural activity at event boundaries in the hippocampus and Posterior Medial network. *Nat Commun* **11**, 3980 (2020).

70. Kullmann, W. Homer and Historical Memory. in *Signs of Orality* 95–113 (Brill, 1999). doi:10.1163/9789004351424_007.

71. Neale, M. *Songlines: The Power and Promise*. (Thames & Hudson Australia, Port Melbourne, Victoria, 2020).

72. Mar, R. A., Li, J., Nguyen, A. T. P. & Ta, C. P. Memory and comprehension of narrative versus expository texts: A meta-analysis. *Psychon Bull Rev* **28**, 732–749 (2021).

73. Goldstein, A. G., Chance, J. E., Hoisington, M. & Buescher, K. Recognition memory for pictures: Dynamic vs. static stimuli. *Bulletin of the Psychonomic Society* **20**, 37–40 (1982).

74. Antony, J., Lozano, A., Dhoat, P., Chen, J. & Bennion, K. Causal and Chronological Relationships Predict Memory Organization for Nonlinear Narratives. *J Cogn Neurosci* **36**, 2368–2385 (2024).

75. Schlaggar, B. L. & McCandliss, B. D. Development of Neural Systems for Reading. *Annual Review of Neuroscience* **30**, 475–503 (2007).

76. Marano, G. *et al.* The Neuroscience Behind Writing: Handwriting vs. Typing—Who Wins the Battle? *Life (Basel)* **15**, 345 (2025).

77. Colombo, D. *et al.* Egocentric and allocentric spatial reference frames in aging: A systematic review. *Neuroscience & Biobehavioral Reviews* **80**, 605–621 (2017).

78. Gross, A. L. *et al.* Do older adults use the Method of Loci? Results from the ACTIVE Study. *Exp Aging Res* **40**, 140–163 (2014).

79. Fealy, S. *et al.* Psychological interventions designed to reduce relocation stress for older people transitioning into permanent residential aged care: a systematic scoping review. *Aging & Mental Health* **28**, 1197–1208 (2024).

80. West, G. L. *et al.* Landmark-dependent Navigation Strategy Declines across the Human Life-Span: Evidence from Over 37,000 Participants. *J Cogn Neurosci* **35**, 452–467 (2023).

81. Smith, D. *et al.* Cooperation and the evolution of hunter-gatherer storytelling. *Nat Commun* **8**, 1853 (2017).

82. Shevlin, H., Vold, K., Crosby, M. & Halina, M. The limits of machine intelligence. *EMBO Rep* **20**, e49177 (2019).

83. Korteling, J. E. (Hans)., van de Boer-Visschedijk, G. C., Blankendaal, R. A. M., Boonekamp, R. C. & Eikelboom, A. R. Human- versus Artificial Intelligence. *Front Artif Intell* **4**, 622364 (2021).

84. Feinberg, D. A. *et al.* Multiplexed Echo Planar Imaging for Sub-Second Whole Brain FMRI and Fast Diffusion Imaging. *PLOS ONE* **5**, e15710 (2010).

85. Moeller, S. *et al.* Multiband multislice GE-EPI at 7 tesla, with 16-fold acceleration using partial parallel imaging with application to high spatial and temporal whole-brain fMRI. *Magn Reson Med* **63**, 1144–1153 (2010).

86. Stigliani, A., Weiner, K. S. & Grill-Spector, K. Temporal Processing Capacity in High-Level Visual Cortex Is Domain Specific. *J Neurosci* **35**, 12412–12424 (2015).

87. Sochat, V. The Experiment Factory: Reproducible Experiment Containers. *Journal of Open Source Software* **3**, 521 (2018).

88. Durnez, J., Blair, R. & Poldrack, R. Neurodesign: Optimal experimental designs for task fMRI. *bioRxiv* 119594 (2018) doi:10.1101/119594.

89. Ghorbani, S. *et al.* MoVi: A large multi-purpose human motion and video dataset. *PLOS ONE* **16**, e0253157 (2021).

90. Glasser, M. F. *et al.* The Minimal Preprocessing Pipelines for the Human Connectome Project. *Neuroimage* **80**, 105–124 (2013).

91. Smith, S. M. *et al.* Resting-state fMRI in the Human Connectome Project. *Neuroimage* **80**, 144–168 (2013).

92. Glasser, M. F. *et al.* The Human Connectome Project's neuroimaging approach. *Nat Neurosci* **19**, 1175–1187 (2016).

93. Jenkinson, M., Beckmann, C. F., Behrens, T. E. J., Woolrich, M. W. & Smith, S. M. FSL. *Neuroimage* **62**, 782–790 (2012).

94. Ardekani, B. A. & Bachman, A. H. Model-based automatic detection of the anterior and posterior commissures on MRI scans. *Neuroimage* **46**, 677–682 (2009).

95. Posse, S. *et al.* Enhancement of BOLD-contrast sensitivity by single-shot multi-echo functional MR imaging. *Magn Reson Med* **42**, 87–97 (1999).

96. Greene, D. J. *et al.* Developmental Changes in the Organization of Functional Connections between the Basal Ganglia and Cerebral Cortex. *J. Neurosci.* **34**, 5842–5854 (2014).

97. Choi, E. Y., Yeo, B. T. T. & Buckner, R. L. The organization of the human striatum estimated by intrinsic functional connectivity. *J Neurophysiol* **108**, 2242–2263 (2012).

98. Kong, R. *et al.* Spatial Topography of Individual-Specific Cortical Networks Predicts Human Cognition, Personality, and Emotion. *Cereb Cortex* **29**, 2533–2551 (2019).

99. Bielczyk, N. Z. *et al.* Thresholding functional connectomes by means of mixture modeling. *NeuroImage* https://doi.org/10.1016/j.neuroimage.2018.01.003 (2018) doi:10.1016/j.neuroimage.2018.01.003.

100. Chauvin, R. J., Mennes, M., Buitelaar, J. K. & Beckmann, C. F. Assessing age-dependent multi-task functional co-activation changes using measures of task-potency. *Dev Cogn Neurosci* https://doi.org/10.1016/j.dcn.2017.11.011 (2017) doi:10.1016/j.dcn.2017.11.011.

101. Chauvin, R. J., Mennes, M., Llera, A., Buitelaar, J. K. & Beckmann, C. F. Disentangling common from specific processing across tasks using task potency. *NeuroImage* **184**, 632–645 (2019).

102. Chauvin, R. J. *et al.* Task-generic and task-specific connectivity modulations in the ADHD brain: an integrated analysis across multiple tasks. *Transl Psychiatry* **11**, 1–10 (2021).

103. Salo, T. Developing and Validating Open Source Tools for Advanced Neuroimaging Research. *FIU Electronic Theses and Dissertations* https://digitalcommons.fiu.edu/etd/5010 (2022).

104. Napoli, N. J., Barnes, L. E., Premaratne, K. & IEEE. Correlation Coefficient Based Template Matching: Accounting for Uncertainty in Selecting the Winner. *2015 18TH INTERNATIONAL CONFERENCE ON INFORMATION FUSION (FUSION)* 311–318 (2015).

105. Markello, R. D. *et al.* neuromaps: structural and functional interpretation of brain maps. *Nat Methods* 1–8 (2022) doi:10.1038/s41592-022-01625-w.

Method

Participants

Memory Champion: The Memory Champion was 31 years of age at the first visit and 37 years of age at the second visit, and practiced memory sports starting in 2010, representing 5 years and 11 years of training for each visit. The Memory Champion is a six-time United States memory champion who holds several current and former U.S. memory records along with the Grand Master of Memory title.

MSC participants: The MSC is composed of 10 neurotypical, right-handed, adult participants (24-34 years of age at the time of testing; 5 females), who were recruited from the Washington University in St. Louis community. Participants completed 10 sessions of scanning that were 1.5 hour each, with all scan sessions completed within 7 weeks. The MSC dataset is publicly

available (https://openneuro.org/datasets/ds000224). Details of the dataset and processing pipeline have been previously described [11].

PFM MRI acquisition

2015 Memory Champion visit and MSC protocol: Data collection and processing pipeline for the Memory Champion followed the MSC protocol acquired in 2013, for the 2015 visit. All participants were scanned on a Siemens TRIO 3T across 12 sessions (2 sessions of structural MRI scans + 10 sessions of functional MRI scans). Structural images included four T1-weighted scans (TE = 3.74ms, TR = 2400ms, TI = 1000ms, flip angle = 8°, 0.8mm isotropic voxels, 224 sagittal slices), four T2-weighted images (TE = 479ms, TR = 3200ms, 0.8mm isotropic voxels, 224 sagittal, 224), four MRA and eight MRV scans, which were not used in the present study.

Functional images included 300 minutes of eyes-open resting-state fMRI BOLD data (10 sessions x 30min/session) using a gradient-echo EPI BOLD sequence (TE = 27ms, TR = 2.2s, flip angle = 90°, 4mm isotropic voxels, 36 axial slices). Gradient echo field map images (one per session) were acquired with the same parameters. See (Gordon et al., 2017) for more details.

2021 Memory Champion visit and MSC02 MSC06 protocol:

Each participant performed multiple MRI acquisition sessions for functional imaging. All participants were scanned on a Siemens TRIO 3 T MRI scanner. For each session, the protocol included a series of task fMRI and resting-state fMRI BOLD data using the CMRR multiband (Mb)-ME sequence[84,85] with five echoes (14.2 ms, 38.93 ms, 63.66 ms, 88.39 ms, 113.12 ms; TR = 1.761 s, 2 mm resolution, MB factor = 6, IPAT = 2, flip angle = 68°). Data was acquired in the PA phase encoding direction. Additionally, spin echo field maps were acquired in both AP and PA directions (SE, single-band, 3 frames per run, TR = 8.0 s, TE = 66 ms, flip angle = 90°).

This resulted in approximately 8 hours of fMRI data: 105 minutes of eyes-open resting-state fMRI BOLD data and 377 minutes of task fMRI for the Memory Champion. Table 1 provides details on the number of available minutes per task per participant. Two tasks were tailored to the specific capacities of the Memory Champion and the performance of the Method of Loci and were not performed by controls. Additionally, the two localizer tasks were acquired to better understand the neural response of the Memory Champion in the Method of Loci task and were acquired with fewer repetitions for controls, as aiming only to validate the spatial pattern reproducibility.

The order of task fMRI acquisition was randomized in each session, with resting-state then deck of card memory task was performed last, in order to score the memorization of the card order immediately after the task, outside of the scanner.

task	MC	MSC02	MSC06
Rest (15 minutes)	7	5	4
Deck of cards memory task (15min)	8	-	-
Pi retrieval (15min)	5	-	-
Reading span (10min)	7	9	8
Stanford VPN Localizer (8 min)	7	-	-

Action localizer (7 min)	8	-	-

Table 1: task and rest available data per participant

fMRI Task

Stanford VPN Localizer:

The Stanford VPN localizer task is a functional localizer experiment used to define category-selective cortical regions[86]. The selected categories were adult face, body, instrument, corridor (labeled space), and digit. The task was performed as a 1-back task within each category block using the Psychopy version available at https://github.com/VPNL/fLoc.

All subsequent tasks were built using JSpsych. The reading span task was adapted from the versions available in the Experiment Factory[87]. Each task and each task repetition within a subject had an independent event or block presentation order, with an event-related design optimized for design efficiency under our 1.761 seconds TR fMRI sequence using NeuroDesign[88]. Tasks were optimized for detection power for all tasks except for the N-back designs, where frequency and confounder parameters were also prioritized to avoid psychological predictability of event presentation. This optimized order and timing of events help maximize the HRF power. See Figure S22 for task schema

Action localizer: The action localizer task was built using the BML-MoVi dataset (Biomotion Lab MoVi: A large multi-purpose human motion and video dataset[89]). The task comprises two different types of blocks: action and non-action blocks, performed as a 1-back task on short video stimuli. In the action blocks, the stimuli were reconstructed 3D body shapes of 13 different subjects performing one of 20 actions, such as crawling or throwing a ball. In the non-action blocks, the same videos were transformed into a vine (back-and-forth repetition) of the first second of the video, reproducing all identical visual characteristics of the original video with body motion perception but without the perception of complete action movement.

Three blocks of each category, including 10 videos each, composed a task run. Videos were followed by a time-jittered fixation cross. Accuracy feedback and repetition of the instructions were provided for 9 seconds between blocks. See Figure S21 for task schema

Reading span task: The reading span task is a working memory task consisting of a memorization phase, a proactive recall phase, and a testing phase, repeated eight times. Each repetition involves a set of words to remember, ranging from four to seven words. Words are presented one at a time for 1.25 seconds, followed by a time-jittered fixation cross and a sentence. Participants are asked to remember the word and then judge whether the subsequent sentence is sensical or not, repeating this process four to seven times. This is followed by a screen marked '???' for 5 seconds during which participants have to proactively recall the list of words they were asked to remember.

Finally, four to seven words are presented one by one on the screen with a question mark, and participants have to judge whether each word was part of the list they had to remember. This is followed by a time-jittered fixation cross. A short screen reading 'new set' indicates the start of a new set, beginning again with the word memorization-sentence judgment alternation for the new set. See Figure S20 for task schema

Deck of cards memory task: The deck of cards memory task aimed to target the neural correlates of the Method of Loci strategy. It comprised multiple sections to contrast the different elements of the strategy. The task begins with the viewing of cards, with instructions to judge whether the card appeared on the left or right side of the screen. Both real and fake cards (with made-up symbols) were used in this section and the following one. Seventy cards were presented for 1 second each, followed by a time-jittered fixation cross. This was followed by the presentation of 72 cards (real or fake) at three positions on the screen, representing the content associated with the card by the Memory Champion: action, person, or object. The Memory Champion was instructed to mentally visualize the associated content. Each card appeared for 2 seconds, spaced 0.5 seconds apart. An 8-second instruction screen informed the Memory Champion of the next section: deck of cards memorization.

A deck of cards was presented 3 cards at a time, as the Memory Champion would visualize them by associating each card with a concept (action, person, and object) into a scene in his memory palace. Each triplet of cards was shown for 6 seconds, spaced 0.3 seconds apart. This section was followed by a 1-minute fixation cross, during which the Memory Champion proactively recalled the order of the deck of cards. The proactive recall section was followed by cued recall and testing. A triplet of cards from the deck just memorized was shown 9 times, and the Memory Champion had 8 seconds to recall the three cards following it in the deck order. Then, a triplet of cards was proposed as a solution, and the Memory Champion had 3 seconds to judge whether it was the correct triplet. This deck of cards memorization, proactive recall, cued recall, and testing sequence was done twice, with a new deck of cards to memorize. The Memory Champion then came out of the scanner and sorted two physical decks of cards in the order of the two decks of cards just memorized. Once both decks were sorted, accuracy was evaluated by the experimental team. See Figure S18 for task schema

Pi retrieval task: As a simulation of a pi challenge, in which the Memory Champion would be asked to find the 5 digits following a given 5 digits within the first 10,000 digits of pi, a task was built to capture the Method of Loci recall strategy. The encoding strategy is similar to the deck of cards method, where an action-person-object association is assigned to each digit, then represented in a scene. The set of 5 digits is separated into the first three digits and the last three digits (with the middle digit represented twice). This results in a scene with two people performing two actions with two objects stored in a large memory palace. The pi retrieval task aims to leverage this already encoded large item to capture the recall strategy in more detail. The task is composed of two sections: a cued recall phase (5 minutes) and a proactive recall phase (10 minutes).

During the first 5 minutes of the task, 5-digit sets within the first 10,000 digits of pi are presented. The presentation of each digit set has three parts: (1) showing the first three digits for 4 seconds, (2) showing the last three digits for 4 seconds, during which the Memory Champion is instructed to compose the scene associated with the digit triplet, and (3) showing the full 5-digit set for 6 seconds, during which the Memory Champion is instructed to localize the scene in his memory palace. This sequence is repeated 15 times for different sets of 5 digits. The Memory Champion could succeed (search+find) or fail (search only) to retrieve the series of digits within the 6 seconds allocated. We specifically contrasted the neural activation during search and successful retrieval of the localization of a 5-digit series from the first 10,000 digits of pi to differentiate networks involved in the longer search process versus localization of the digits.

This is followed by the proactive recall phase: a 10-minute fixation cross period during which the Memory Champion is instructed to recall the digits of pi in order from the start. See Figure S19 for task schema

HCP datasets and processing: We used data from 887 participants aged 22-35 years (410 female) from the HCP 1200 participants release[44], each with 60 minutes of resting-state fMRI. A custom Siemens SKYRA 3.0T MRI scanner and a custom 32-channel head matrix coil were used to obtain high-resolution T1-weighted (MP-RAGE, TR = 2.4 s, 0.7 mm³ voxels) and BOLD contrast-sensitive (gradient-echo EPI, multiband factor 8, TR = 0.72 s, 2 mm³ voxels) images from each participant. BOLD acquisition included a left-to-right or right-to-left phase encoding, performed for 15 minutes of resting state twice for each participant. Data was downloaded from https://db.humanconnectome.org and used the standard HCP preprocessing pipeline[90], which includes similar steps to our PFM preprocessing pipeline. For more information on acquisition and processing, see [44,68,90–92].

PFM MRI preprocessing

Structural: Cortical surfaces were generated according to the procedures described in [21]. Each participant's averaged T1-weighted image, after field inhomogeneity correction by FSL FAST [93], was processed through the FreeSurfer recon-all pipeline to anatomically segment and label the amygdala, accumbens, caudate, cerebellum, hippocampus, pallidum, putamen, and thalamus in both hemispheres. This segmentation was used to create subcortical masks and anatomical surfaces for transforming the functional data into CIFTI format. The surfaces were then registered into fs_LR_32k surface space using the Multi-modal Surface Matching algorithm [68]. Volumes were also registered to MNI152 space.

Caudate segmentation: The caudate was segmented into head and body segments using anterior commissure-posterior commissure (AC-Pc) alignment via ACPC Detect[94]. Coronal slices of the AC and PC were used to delimit the end of the head and the beginning of the body segments within the caudate structure, which was segmented by FreeSurfer. The tail segment, located posterior to the PC slices, was not represented for all participants, as the caudate tail is a thin and elongated structure that might require higher resolution for accurate capture in some individuals. Therefore, analyses were performed only for the head and body segments of the caudate.

Functional preprocessing: Functional preprocessing follows the previously described pipeline of the MSC dataset [21] and involved temporal interpolation to correct for differences in slice acquisition timing, rigid-body correction of head movements, correction for susceptibility inhomogeneity-related distortions using field maps, and alignment to MNI152 space. For multi-echo data, echoes were optimally combined using the T2*-based echo weighting combination method[95] . Processing was done using 4dfp tools (https://readthedocs.org/projects/4dfp/).

Signal to noise ratio mask: Signal-to-noise ratio (SNR) is calculated on the data before noise regression as the average signal overtime divided by variance of signal overtime for each run. We used a SNR mask to remove region of low signal for the analysis. In the 2015 datasets, we use the average mask defined with the MSC data to maintain comparability with previous analysis with the MSC datasets. For the 2021 datasets, we define a SNR mask for each individual, as region with SNR above 20.

Resting state fMRI preprocessing: Resting state fMRI (resting state fMRI) data denoising involved the removal of high-motion frames (framewise displacement [FD] > 0.1 mm for the single echo and FD > 0.16 mm after low-pass filtering at 0.1 Hz), band-pass filtering (0.005 to 0.1 Hz), and regression of nuisance time series, including head movement parameters, the global signal (averaged and derivative across all gray-matter voxels), and orthogonalized waveforms extracted from ventricles, white matter, and extracranial tissues. The resting state fMRI data was then projected to the cortical surface as the last step. The data were smoothed using a two-dimensional 6-mm full-width half-maximum (FWHM) smoothing kernel. Additionally, to mitigate the effects of signal contamination from nearby cortical areas in the subcortex, the average time series of all cortical vertices within 20 mm of a subcortical voxel was included as a regressor to clean the subcortical volume, similar to strategies used in previous work on subcortical functional connectivity[96,97].

Task-fMRI preprocessing: Task fMRI data were low-pass filtered at 0.1 Hz. The task fMRI data was then projected to the cortical surface. Task analyses were performed in grayordinates, following the HCP pipeline. The same nuisance time series described for resting state fMRI were selected and included in the FSL-based GLM analysis as confounds. Frames with high head movement were identified and each was included as an individual column in the confound matrix of the GLM. Only the resulting cortical surfaces from the task analysis were smoothed using a two-dimensional 6-mm full-width half-maximum (FWHM) smoothing kernel.

fMRI processing

FMRI Task analysis: Task block designs and event-related designs were modeled using a double gamma HRF in a GLM analysis with FSL FEAT [32]. Analysis was conducted independently on surface and subcortical grayordinates, following the HCP pipeline steps (release v4.3). Second-level analysis across runs within participants was performed using FSL, and the resulting z-scores were used to compare effects. Only positive BOLD activity was considered and displayed.

Network individual boundaries (MSHBM): To define individual-specific network boundaries, the multi-session hierarchical Bayesian model (MS-HBM) method[98] was used for each participant and each dataset. This method differentiates intra-subject (within-subject) from inter-subject (between-subject) network variability, which helps with a robust estimation of individual network boundaries. An 18-functional network identity template (Default Mode, Context Association, Visual-Lateral, Visual-Dorso-ventral Stream, Visual Primary, Visual Middle Temporal, Frontoparietal, Dorsal Attention, Peri-motor, Language, Salience, Action-mode, Parietal Memory, Auditory, Motor-Hand, Motor-Face, Motor-Foot, Auditory and Somato-Cognitive-Action), derived from [41], was used to inform the final step of network labeling.

FC quantification: Grayordinates from regions of interest or networks were used to average BOLD fMRI activity into time series. These time series were then used as seeds to calculate either full brain correlation maps or as nodes to calculate correlations between networks and regions. For seed map functional connectivity, all resting-state fMRI runs were concatenated, while resting-state fMRI runs were kept separate for run-specific FC, which was then used for testing group differences. For all analyses comparing the Memory Champion to the HCP population, the atlas template network borders were used to calculate the network FC maps for the Memory Champion and for each individual in the HCP dataset. For all analyses comparing

the Memory Champion to controls with Precision Functional Mapping data, individual-specific network borders were used for analysis.

Module analysis: Seed FC maps from the specific FC region of the Memory Champion were calculated from the concatenated resting-state and Method of Loci state (from the second part of the pi retrieval task). When the Method of Loci and the resting-state FC are compared, the resting-state FC is calculated on a matching length of acquisition, i.e., the first 10 minutes of the resting state. Spatial correlations between seed maps were calculated and used to perform hierarchical clustering using the Ward algorithm to order the regions. The resulting hierarchical order from the resting-state seed maps is used consistently throughout the manuscript to display results of the specific regions. Tests of the significance of the similarity between the specific regions' seed maps were performed against the correlation similarity of 1,000 random seed maps with matching sizes to each of the specific seed regions. Random seeds were generated using Moran randomization to account for the spatial constraints of the individual brain on the surface projection and the volume mask. A z-score and percent correlation beyond the random distribution is presented in the supplement and shows larger similarities than random forming clusters. A principal component analysis was also performed across the specific seed maps to validate the signal separation across different components, replicating the three modules within the first three components.

FC testing in PFM dataset: Resting-state run-specific FC values were tested for differences between the Memory Champion and controls and corrected within datasets. For each region (anatomically or functionally defined) of interest, networks with positive FC connections to that region in the Memory Champion were considered for testing using independent t-tests and included in the False Discovery Rate (FDR) correction. For full network-to-network testing, all positive network-to-network connections were tested and corrected for FDR. Similarly, for full subcortical-to-network testing, all positive subcortical-to-network connections were included in the FDR correction. Identically, FC differences between network-to-network and subcortical-to-network positive connections were estimated at the run-specific level to compare resting-state and pi retrieval (Method of Loci) state FCs, and were FDR corrected. Significance was determined at $p=0.05$ after correction.

Specificity and centrality analysis with HCP data

Gaussian Noise FC normalization:

To compare FC between our datasets, in which the distribution of values is skewed differently due to differences in fMRI sequence, the number of volumes available, and preprocessing choices, we perform a mixture modeling normalization of the FC. This method is an adaptation of a technique used in previous functional connectivity studies to compare FC[99–102]. The method aims to model the Gaussian noise independently of the FC signal from the tails of the distribution, in order to normalize the FC distribution by the Gaussian noise distribution. To achieve this, we aggregate all FC network maps for a subject to obtain a brain wide fully defined FC distribution and perform a Gaussian-Gamma mixture model. The two-tailed gamma distributions capture the FC signal, while the main Gaussian captures the noise. The mean and deviation of the Gaussian distribution are then used to scale the FC distribution. The individually specific rescaled FC network maps allow a more accurate comparison of network FC maps across individuals. This scaling is done at the structure level (cortex, and each FreeSurfer-segmented subcortical structure from the subcortical mask) to better address signal differences

between sequence and scanner, especially different signal quality in the subcortex. This rescaling is performed for each individual in the HCP dataset and the PFM datasets and results in Z score FC maps.

High centrality detection: Once the rescaled FC network maps are obtained for each individual, the rescaled network FC maps of the Memory Champion are compared to each map of the HCP participants. Quantification of the percentage of HCP FC maps below the FC values of the Memory Champion is performed at the grayordinate level. This results in a ratio describing how specifically strong the Memory Champion's FC is locally for each network in our template. This quantification is performed for both visits of the Memory Champion, and for replication, the Memory Champion's rescaled FC strength from the 2015 specificity ratio is also calculated relative to the rescaled FC from the MSC subjects. Regions with FC beyond 95% of controls are selected for further analysis. Regions selected for more than one network and larger than 20 vertex/voxels are defined as high centrality regions.

Neurosynth analysis: To characterize the functional role of specific regions, we explore the Neurosynth [49] terms maps, which are statistical maps grouping references of neural activation through automated literature review. We used NiMare[103] to download the terms maps and removed all terms that were related to anatomy, functional network, disorders, and conjunction words. Each map was max scaled and the mean value of voxels from each of the high centrality memory champion regions or from the combined voxels of regions within a cortical module was calculated. The 15 terms with the highest values were selected and displayed in a cloud map with font size weighted by the term average value using the wordcloud python package.

Winner-take-all network representation in subcortex: To determine where networks are represented in the subcortex and to create a consensus map, a winner-take-all analysis is performed across average network maps for the HCP population and MSC participants. Average network maps are calculated from the rescaled FC maps to better adjust for variation in noise between subjects in each dataset. The network with the highest FC value is identified as the winner for a given grayordinate, resulting in maps with network labels for both the HCP population and MSC participants.

Network territory in subcortex: While the winner-take-all approach provides a condensed visual summary, it masks the richness of network representation under the winning network. To quantify the overlap of the specificity pattern with the network representation in the subcortex, we opted to quantify the overlap with network territories. To account for uncertainty in the selection of the winner, we used a Dempster-Shafer theoretic model, as presented in[104], to weigh the representation of each network at each voxel and evaluate which networks are competitors to the winning network. This results in a map for each network, delineating regions where network connectivity is strongly represented and competing for the winner labeling, which we refer to as network territory.

Spatial Significant testing: To evaluate whether a result is significantly spatially represented in a cortical network or subcortical structure, results are tested against null distribution maps built using the Moran randomization strategy [105]. This randomization is constrained by spatial distance in the data, enabling us to test both cortical and subcortical spatial results with the same algorithm. Spatial randomization can be built relative to each individual brain's spatial constraints, which is highly appropriate for precision functional mapping analysis, as previously demonstrated in [40].

After building 1000 randomized maps that respect the distribution value of the result under evaluation, average values are calculated for non-thresholded maps per individual-specific network borders and subcortical structures. For thresholded maps, the percentage overlap of the result with network and subcortical structures is calculated. A p-value is then calculated by comparing the true value to the random maps' distribution values. These p-values are corrected for multiple comparisons across networks and subcortical structures using FDR.

Non-thresholded map analyses correspond to task contrast. Thresholded map analysis corresponds to the specificity maps testing, thresholded at 95%, and the Memory Champion memory networks specificity overlap with controls network territories in the subcortex. For the specificity to network territory testing, the overlap is calculated over the entire subcortical representation of the network territory, not by individual subcortical structure, to simplify the interpretation.